Global change in terrestrial ecosystem detected by fusion of microwave and optical satellite observations

Running title: global land change by microwave and optical observations

Hideharu Nara[1+], Yohei Sawada[2+],

[1] Department of Civil Engineering, the University of Tokyo, Tokyo, Japan

[2] Institute of Engineering Innovation, the University of Tokyo, Tokyo, Japan

+These authors have equally contributed and should be considered as co-first authors.

manuscript to be submitted to *Geophysical Research Letters*

Corresponding author: Y. Sawada, Institute of Engineering Innovation, the University of Tokyo, Tokyo, Japan, 2-11-6, Yayoi, Bunkyo-ku, Tokyo, Japan, yohei.sawada@sogo.t.u-tokyo.ac.jp

Abstract

The detection and quantification of global land change by satellite observations are the grand challenges to improve the understanding of global environmental change. In this study, we develop a new vegetation index, which can be used as a proxy of the fractions of tree canopy and short vegetation, based on the simple linear regression between microwave vegetation optical depth (VOD) and optical leaf area index (LAI). Although we use no high-resolution reference data, the newly developed vegetation index successfully detects and quantifies the global land change which has been reported by the previous estimations based on high-resolution reference data. We find that the relationship between VOD and LAI is non-stationary and the temporal change in the VOD-LAI relationship is the important signal to detect and quantify global change in the terrestrial ecosystem.

Plain language summary

The detection and quantification of global land change, such as deforestation and afforestation, are crucially important to understand the effects of climate change and human activities on the terrestrial ecosystem. There are two major methodologies of satellite remote sensing of vegetation: optical and microwave remote sensing. While

photosynthetic activities of plants can be observed by optical remote sensing, total aboveground vegetation water content can be observed by microwave remote sensing. Here we find that the simple linear regression between two vegetation indices generated from optical and microwave satellite observations can accurately quantify the fractions of tree canopy and short vegetation in the observation pixels. We apply this finding to detect global land change from 2003 to 2019. We can detect several important land changes, such as tree canopy gain in Sahel and deforestation in southeastern Amazon.

Key Points

1. The simple linear regression between VOD and LAI can quantify the fractions of tree canopy and short vegetation/bare ground.

2. The relationship between VOD and LAI is non-stationary and its temporal change is the important signal to detect global land change.

1. Introduction

The detection and quantification of global change in the terrestrial ecosystem are crucially important to understand global environmental change. Vegetation indices generated from optical satellite observations (e.g., Zhu et al. 2013; Tucker et al. 2005) have been intensively used to monitor the change in the terrestrial ecosystem. For example, Song et al. (2018) developed a yearly global vegetation product, in which every land pixel is characterized by its per cent cover of tree canopy, short vegetation, and bare ground, from the optical-infrared Normalized Difference Vegetation Index (NDVI), and successfully detected the long-term global land change.

59 The limitation of the optical satellite observation is that it is sensitive only to a
60 photosynthetically active part of terrestrial biomass (i.e. leaf) and it is not
61 straightforward to retrieve the amount of a photosynthetically inactive part of
62 aboveground biomass (i.e. woody biomass). To distinguish tree canopy and short
63 vegetation from optical satellite observations, complex supervised machine learning
64 with high-resolution reference data is usually required (e.g., Song et al. 2018). To
65 overcome this limitation, microwave remote sensing has been recognized as an
66 alternative approach to monitor global change in the terrestrial ecosystem. Microwave
67 Vegetation Optical Depth (VOD) is sensitive to vegetation water content, which
68 includes the information of both leaf and woody biomass (see Owe et al. (2001) and
69 Jones et al. (2011) for the detailed description of VOD and the retrieval algorithms). Liu
70 et al. (2015) successfully monitored the long-term change in global aboveground
71 biomass carbon by microwave VOD data. Zhou et al. (2014) indicated that microwave
72 VOD was more sensitive to the degradation of the Congo rainforest by drought than the
73 optical vegetation index.
74
75 Combining the microwave and optical vegetation indices has the potential to improve
76 the understanding of vegetation dynamics. Jones et al. (2013) found that the post-fire

77 recovery of NDVI was much faster than that of microwave VOD, which indicated the
78 faster recovery of short vegetation than woody biomass after extreme wildfires in
79 Alaska and Canada. Van Dijk et al. (2013) found that in the Australian millennium
80 drought, no decreasing trend could be detected in the optical vegetation indices while
81 microwave VOD significantly declined. By numerical simulation, Sawada and Koike
82 (2016) attributed this difference to the higher resilience of short vegetation to drought
83 than woody biomass. These studies showed the high potential of fusions of microwave
84 and optical satellite observations to distinguish the dynamics of tree canopy and short
85 vegetation.
86
87 We aim to develop a new method to detect global land change by combining microwave
88 VOD and optical Leaf Area Index (LAI). We reveal that the simple linear regression
89 between microwave VOD and optical LAI provides a useful proxy of the fractions of
90 tree canopy and short vegetation. The proposed vegetation index successfully detects
91 and quantifies global change in the terrestrial ecosystem from 2003 to 2019 without any
92 additional reference data.
93
94

2. Data

We used the microwave VOD product based on the Land Parameter Retrieval Model (LPRM) provided by National Aeronautics and Space Administration (NASA). The description of the LPRM algorithm can be found in Owe et al. (2001) and Owe et al. (2008). Microwave VOD is retrieved from C-band (6.9 GHz) brightness temperature observed by Advanced Microwave Scanning Radiometer for Earth observation system (AMSR-E) and AMSR2. The VOD products from both AMSR-E (from June 2002 to September 2011) and AMSR2 (from July 2012 to December 2019) were used. We used only night scene data to reduce the effect of a surface temperature bias in the retrieval algorithm (Liu et al. 2011). The spatial resolution of this dataset is 0.25 degree. The temporal resolution of this dataset is approximately 2-daily, and we resampled it to 8-daily.

We used the optical LAI product processed by Ichii et al. (2017). Ichii et al. (2017) applied detailed quality control to MODerate resolution Imaging Spectroradiometer (MODIS) onboard Terra and Aqua satellites LAI L4 data (MCD15A2H; Myneni et al. 2015). The spatial and temporal resolutions are 0.25 degree and 8-daily, respectively.

As land cover data, we used the MODIS land cover climate modeling grid (MCD12C1) version 6 data product (Friedl et al. 2015). The temporal resolution of this dataset is yearly. The original spatial resolution of this dataset is 0.05 degree and we resampled it to 0.25 degree by the nearest neighbor approach.

3. Method

The Microwave and Optical Fusion Approach (MiOFA) was originally proposed by Sawada et al. (2017a) to improve the skill to retrieve surface soil moisture and vegetation water content from C-band brightness temperature. In the MiOFA, the relationship between VOD and total aboveground Vegetation Water Content (VWC) can be formulated as:

$$VOD = b \times VWC + R \quad (1)$$

where b is a parameter and R quantifies the effect of surface soil roughness. Because it is difficult to distinguish the effects of vegetation and surface soil roughness on brightness temperature, the existing VOD data include the effect of surface soil roughness (e.g., Sawada et al. 2016, 2017a, 2017b; Wang et al. 2015; Njoku and Chan 2006). The important assumption of the MiOFA is that b-parameter for C-band VOD is

time-invariant and species-independent. Sawada et al. (2016) and Sawada et al. (2017b) supported this assumption by a field experiment although Jackson and Schmugge (1991) originally formulated this parameter as a species-dependent variable.

Paloscia and Pampaloni (1988) proposed the empirical relationship between VWC and optical LAI, which was supported by the in-situ observations (e.g., Sawada et al. 2017b):

$$VWC = \exp\left(\frac{LAI}{y}\right) - 1 \cong \frac{LAI}{y} \quad (2)$$

where y is a species-dependent parameter which cannot be directly observed by satellite sensors. The y-parameter can be recognized as the contribution of leaf biomass to the total aboveground VWC. The lower y indicates the larger fraction of short vegetation since the small increase of LAI induces the large increase of total aboveground VWC. The higher y indicates that there is the larger amount of tree canopy. The y-parameter can be a good index of canopy biomass structure.

By substituting (2) to (1), we obtain the equation (3).

$$VOD = \frac{b}{y} LAI + R \quad (3)$$

148 The MiOFA proposes to estimate the parameters of canopy biomass structure (b/y) and
149 surface soil roughness (R) by the linear regression between microwave VOD and optical
150 LAI. In the original paper of the MiOFA (Sawada et al. 2017a), the R-parameter was
151 focused on to improve the retrieval of surface soil moisture. In this paper, we focused on
152 the slope of the linear regression, b/y, as a vegetation index. Because we assumed that b
153 is a constant parameter, we hypothesized that tree canopy (short vegetation) is dominant
154 in pixels with lower (higher) b/y.
155
156 By performing the linear regression between microwave VOD and optical LAI, we
157 developed the yearly global b/y dataset from 2003 to 2019. Since we had no C-band
158 brightness temperature observations in the transition period from AMSR-E to AMSR2,
159 we did not estimate b/y in 2011 and 2012 (see also section 2). There are long-term and
160 temporally continuous VOD datasets derived by merging the multi-sensor VOD
161 products (e.g., Moesinger et al. 2020). However, the assumption of the constant
162 b-parameter is correct only in the lower frequencies such as C-band so that we avoided
163 to use VOD retrieved by brightness temperature with higher frequencies in this first
164 application. No significant inconsistency between AMSR-E and AMSR2 has been found
165 in the previous calibration studies (e.g., Okuyama and Imaoka 2015; Parinussa et al.

2015; Du et al. 2017). We showed b/y in the pixels where the slope of the linear regression is positive and statistically significant with a 95% confidence level.

4. Results and discussion

Figure 1 shows climatologic b/y from 2003 to 2019. We use all 8-daily data of microwave VOD and optical LAI in the study period to perform the linear regression, and the estimated slope is shown in Figure 1. Although the linear relationship between microwave VOD and optical LAI is statistically insignificant in the rainforest regions due to the saturation of the signals of VOD and/or LAI in the densely vegetated areas, we can retrieve b/y in most of the vegetated pixels. Generally, b/y tends to be low in the temperate and boreal forest areas. In semiarid grassland, b/y is relatively high indicating the large contribution of LAI to VWC. The spatial distribution of the retrieved R-parameter shown in Figure S1 is similar to the previous global estimation of a roughness parameter in a radiative transfer model (Wang et al. 2015).

To confirm that b/y can be used as the proxy of the fractions of tree canopy and short vegetation, we estimated yearly b/y and compared it with the yearly land cover type

data. Figures 2 and S2 indicate that we obtain low b/y in broadleaf and needleleaf forest areas. b/y increases in savannas, cropland, and grassland areas. In pixels with lower (higher) b/y, tree canopy (short vegetation) is dominant so that our proposed b/y can be a useful index to quantify the fractions of tree canopy and short vegetation. It is not straightforward to distinguish tree canopy dominant pixels from short vegetation dominant pixels by simply analyzing yearly optical LAI (Figure S3). Boxplots in Figure 2 show the large variance of b/y in the specific land cover types probably due to the coarse resolution of microwave VOD, which prevents the direct matchup of b/y with the land cover data (see also section 2).

We can detect global land change by our yearly b/y. Figure 3 shows the linear trend of yearly b/y from 2003 to 2019. The decrease of b/y (shown in blue) indicates the increase of tree canopy, and the increase of b/y (shown in red) indicates the increase of short vegetation/bare ground. Most of the detected trends are consistent to the previous findings. We can detect the increase of tree canopy in the Sahel region, which previous studies attributed to the increase of rainfall (Brandt et al. 2017: Hickler et al. 2005). The increase of tree canopy in eastern Europe detected in our dataset is consistent to previous studies (e.g., Potapov et al. 2015; Hansen et al. 2013). We can detect the

202 widespread increase of tree canopy in China, which resulted from reforestation and
203 afforestation programs (e.g., Piao et al. 2015). The decreasing trend of b/y is also
204 detected in western India, which can be attributed to the transition from bare ground to
205 short vegetation by agricultural activities (Tian et al. 2014). The decrease of tree canopy
206 in southeastern Amazon and Siberia detected in our dataset is also consistent to the
207 previous findings (e.g., Hansen et al. 2013).
208
209 The global land change detected by our newly developed b/y index is consistent to the
210 state-of-the-art dataset provided by Song et al. (2018). Song et al. (2018) estimated the
211 long-term trend of the fractions of tree canopy, short vegetation, and bare ground from
212 NDVI by supervised machine learning with high-resolution reference data. It is
213 promising that our proposed method can detect the similar change in the terrestrial
214 ecosystem to Song et al. (2018) by the simple linear regression between microwave
215 VOD and optical LAI without any reference data. However, there are some differences
216 between changes detected by this study and Song et al. (2018). Song et al. (2018)
217 detected the short vegetation gain in the Congo rainforest, which we do not detect. Song
218 et al. (2018) detected the tree canopy gain in eastern U.S. while the long-term trend in
219 this region is unclear in our dataset. Our estimated trend in Siberia is also inconsistent to

220 Song et al. (2018) although it is consistent to the other estimation which focused only
221 on forest cover (Hansen et al. 2013). There are several reasons for these differences.
222 First, the linear regression between microwave VOD and optical LAI is insignificant in
223 densely vegetated areas as shown in Figure 1 so that our b/y index cannot accurately
224 quantify vegetation dynamics in the dense rainforest. Second, the study period in this
225 study (2003-2019) is different from that in Song et al. (2018) (1982-2016). The human
226 influence on the terrestrial ecosystem in the 20^{th} century cannot be detected in our
227 dataset. Third, the spatial resolution of our b/y data (0.25 degree) is much lower than
228 that of Song et al. (2018) (0.05 degree) so that many impacts of human activities on
229 vegetation dynamics in small scales may be invisible in our data.
230
231 The results shown above imply that the empirical equations and assumptions of the
232 MiOFA described in section 3 are accurate in the global scale. Since these empirical
233 equations and assumptions are closely related to the algorithms to retrieve surface soil
234 moisture and VOD from brightness temperature (e.g., Owe et al. 2001, 2008; Fujii et al.
235 2009; Sawada et al. 2017a) and to assimilate brightness temperature into land surface
236 models (e.g., Yang et al. 2007, 2009; Sawada and Koike 2014; Sawada et al. 2015), our
237 retrieved b/y and R parameters may greatly contribute to improving these algorithms

and the understanding of microwave radiative transfer in the canopy. The most important implication of this study is that the relationship between microwave VOD (or VWC) and the optical vegetation index is non-stationary although it is assumed to be stationary in previous studies on the development and validation of the VWC retrieval algorithms (e.g., Gao et al. 2015). The temporal change in the VOD-LAI relationship is the important signal to quantify global environmental change so that it should not be neglected in the development, validation, and analysis of satellite land observation products.

5. Conclusions

We propose the new vegetation index by combining microwave VOD and optical LAI. Our new index can be the good proxy of the fractions of tree canopy and short vegetation and is useful to detect and quantify global change in the terrestrial ecosystem. The advantage of our new method is that the vegetation index can be obtained by the simple linear regression between microwave VOD and optical LAI so that no high-resolution reference data are required. The limitation is the lower spatial resolution than the other existing methods. Future work will focus on the applications of this new

vegetation index to deepen the understanding of vegetation dynamics in extreme climate conditions such as drought.

Acknowledgement

YS designed the study. HN performed the analysis. HN and YS jointly interpreted the results. YS wrote the first draft of the paper and HN contributed to editing it. This study was supported by JAXA grant ER2GWF102 and JSPS KAKENHI grant 18H03800. The microwave VOD data can be downloaded at https://disc.gsfc.nasa.gov/datasets/LPRM_AMSR2_A_SOILM3_001/summary. The optical LAI data can be downloaded at ftp://modis.cr.chiba-u.ac.jp/ichii/DATA/MODIS/. The land cover data can be downloaded at https://lpdaac.usgs.gov/products/mcd12c1v006/.

References

Brandt, M., et al. (2017), Human population growth offsets climate-driven increase in woody vegetation in sub-Saharan Africa., *Nature Ecology & Evolution, 1*, 0081, https://doi.org/10.1038/s41559-017-0081

Du, J., Kimball, J. S., Jones, L. A., Kim, Y., Glassy, J., & Watts, J. D. (2017), A global satellite environment data record derived from AMSR-E and AMSR2 microwave

Earth observations, *Earth System Science Data, 9,* 791-808, https://doi.org/10.5194/essd-9-791-2017.

Friedl, M. & Sulla-Menashe, D. (2015), MCD12C1 MODIS/Terra+Aqua Land Cover Type Yearly L3 Global 0.05Deg CMG V006. distributed by NASA EOSDIS Land Processes DAAC, https://doi.org/10.5067/MODIS/MCD12C1.006.

Fujii, H., Koike, T., & Imaoka, K. (2009). Improvement of the AMSR-E algorithm for soil moisture estimation by introducing a fractional vegetation coverage dataset derived from MODIS data., *Journal of the Remote Sensing Society of Japan, 29*, 282-292., https://doi.org/10.11440/rssj.29.282

Gao, Y., Walker, J. P., Allahmoradi, M., Monerris, A., Ryu, D., & Jackson, T. J. (2015), Optical Sensing of Vegetation Water Content : A Synthesis Study, *IEEE Journal of Selected Topics in Applied Earth Observations and Remote Sensing, 8*, 1456-1464, https://doi.org/10.1109/JSTARS.2015.2398034.

Hansen, M. C. et al. (2013), High-Resolution Global Maps of 21st-Century Forest Cover Change, *Science, 342,* 850-853, https://doi.org/10.1126/science.1244693.

Hickler, T., Eklundh, L., Seaquist, J. W., Smith, B., Ardö, J., Olsoon, L., Sykes, M. T., and Sjöström, M. (2005), Precipitation controls Sahel greening trend, *Geophysical Research Letters, 32*, L21415, doi:10.1029/2005GL024370.

Ichii, K., et al. (2017), New data-driven estimation of terrestrial CO_2 fluxes in Asia using a standardized database of eddy covariance measurements, remote sensing data, and support vector regression, *Journal of Geophysical Research Biogeosciences.*, 122, 767– 795, doi:10.1002/2016JG003640.

Jackson, T. J., & Schmugge, T. J. (1991). Vegetation effects on the microwave emission of soils. *Remote Sensing of Environment, 36(3)*, 203–212. https://doi.org/10.1016/0034-4257(91)90057-D

Jones, M. O., Jones, L. a., Kimball, J. S., & McDonald, K. C. (2011). Satellite passive microwave remote sensing for monitoring global land surface phenology. *Remote Sensing of Environment*, *115*(4), 1102–1114. https://doi.org/10.1016/j.rse.2010.12.015

Jones, M. O., Kimball, J. S., & Jones, L. A. (2013). Satellite microwave detection of boreal forest recovery from the extreme 2004 wildfires in Alaska and Canada, *Global Change Biology, 19(10)*, 3111–3122. https://doi.org/10.1111/gcb.12288

Liu, Y. Y., De Jeu, R. a M., McCabe, M. F., Evans, J. P., & Van Dijk, A. I. J. M. (2011). Global long-term passive microwave satellite-based retrievals of vegetation optical depth. *Geophysical Research Letters*, *38*(18), 1–6. https://doi.org/10.1029/2011GL048684

Liu, Y. Y., van Dijk, A. I. J. M., de Jeu, R. a. M., Canadell, J. G., McCabe, M. F., Evans, J. P., & Wang, G. (2015). Recent reversal in loss of global terrestrial biomass. *Nature Climate Change*, *5*, 470–474, https://doi.org/10.1038/nclimate2581

Moesinger, L., Dorigo, W., de Jeu, R., van der Schalie, R., Scanlon, T., Teubner, I., & Forkel, M. (2020), The global long-term microwave Vegetation Optical Depth Climate Archive (VODCA), *Earth System Science Data, 12,* 177-196, https://doi.org/10.5194/essd-12-177-2020

Myneni, R., Knyazikhin, Y. & Park T. (2015), MOD15A2H MODIS/Terra Leaf Area Index/FPAR 8-Day L4 Global 500m SIN Grid V006. distributed by NASA EOSDIS Land Processes DAAC, https://doi.org/10.5067/MODIS/MOD15A2H.006.

Njoku, E. G., & Chan, S. K. (2006). Vegetation and surface roughness effects on AMSR-E land observations, *Remote Sensing of Environment, 100(2)*, 190–199. https://doi.org/10.1016/j.rse.2005.10.017

Okuyama, A. & Imaoka, K. (2015), Intercalibration of Advanced Microwave Scanning Radiometer-2 (AMSR2) Brightness Temperature, *IEEE Transactions on Geoscience and Remote Sensing*, *53,* 4568-4577, https://doi.org/10.1109/TGRS.2015.2402204

Owe, M., De Jeu, R., & Walker, J. (2001). A methodology for surface soil moisture and vegetation optical depth retrieval using the microwave polarization difference index. *IEEE Transactions on Geoscience and Remote Sensing*, *39*(8), 1643–1654. https://doi.org/10.1109/36.942542

Owe, M., de Jeu, R., & Holmes, T. (2008). Multisensor historical climatology of satellite-derived global land surface moisture. *Journal of Geophysical Research: Earth Surface*, *113*(1), 1–17. https://doi.org/10.1029/2007JF000769

Paloscia, S., & Pampaloni, P. (1988). Microwave polarization index for monitoring vegetation growth. *IEEE Transactions on Geoscience and Remote Sensing, 26(5)*, 617–621. https://doi.org/10.1109/36.7687

Parinussa, R. M., Holmes, T. R. H., Wanders, N., Dorigo, W. A., & de Jeu, R. A. M. (2015) A Preliminary Study toward Consistent Soil Moisture from AMSR2. *Journal of Hydrometeorology*, *16*, 932–947, https://doi.org/10.1175/JHM-D-13-0200.1.

Piao, S., et al. (2015), Detection and attribution of vegetation greening trend in China over the last 30 years. *Global Change Biology, 21,* 1601-1609. https://doi.org/10.1111/gcb.12795

Potapov, P. V., Turubanova, S. A., Tyukavina, A., Krylov, A. M., McCarty, J. L., Radeloff, V. C. & Hansen, M. C. (2015), Eastern Europe's forest cover dynamics from 1985 to 2012 quantified from the full Landsat archive, *Remote Sensing of Environment, 159,* 28-43, https://doi.org/10.1016/j.rse.2014.11.027.

Sawada, Y., & Koike, T. (2014). Simultaneous estimation of both hydrological and ecological parameters in an ecohydrological model by assimilating microwave signal., *Journal of Geophysical Research, 119*, 8839-8857, https://doi.org/10.1002/2014JD021536

Sawada, Y., Koike, T., & Walker, J. P. (2015). A land data assimilation system for simultaneous simulation of soil moisture and vegetation dynamics. *Journal of Geophysical Research, 120*, 5910-5930, https://doi.org/10.1002/2014JD022895

Sawada, Y. & Koike, T. (2016), Ecosystem resilience to the Millennium drought in southeast Australia (2001–2009), *Journal of Geophysical Research Biogeosciences*, *121*, 2312– 2327, doi:10.1002/2016JG003356.

Sawada, Y., Tsutsui, H., Koike, T., Rasmy, M., Seto, R., & Fujii, H. (2016). A field verification of an algorithm for retrieving vegetation water content from passive microwave observations. *IEEE Transactions on Geoscience and Remote Sensing, 54(4),* 2082-2095, https://doi.org/10.1109/TGRS.2015.2495365

Sawada, Y., Koike, T., Aida, K., Toride, K., & Walker, J. P. (2017a). Fusing Microwave and Optical Satellite Observations to Simultaneously Retrieve Surface Soil Moisture, Vegetation Water Content, and Surface Soil Roughness. *IEEE Transactions on Geoscience and Remote Sensing*, *55*(11), 6195-6206, https://doi.org/10.1109/TGRS.2017.2722468

Sawada, Y., Tsutsui, H., & Koike, T. (2017b), Ground Truth of Passive Microwave Radiative Transfer on Vegetated Land Surfaces. *Remote Sensing., 9,* 655, https://doi.org/10.3390/rs9070655

Song, X.-P., Hansen, M. C., Stehman, S. V., Potapov, P. V., Tyukavina, A., Vermote, E. F., & Townshend, J. R. (2018). Global land change from 1982 to 2016. *Nature*, *560,* 639-643, https://doi.org/10.1038/s41586-018-0411-9

Tian, H., Banger, K., Bo, T., Dadhwal, V. K. (2014), History of land use in India during 1880–2010: Large-scale land transformations reconstructed from satellite data and historical archives, *Global and Planetary Change, 121,* 78-88, https://doi.org/10.1016/j.gloplacha.2014.07.005

Tucker, C. J. et al. (2005), An extended AVHRR 8 - km NDVI dataset compatible with MODIS and SPOT vegetation NDVI data, *International Journal of Remote Sensing, 26,* 4485-4498, https://doi.org/10.1080/01431160500168686

Van Dijk, A. I. J. M., et al. (2013). The Millennium Drought in southeast Australia (2001-2009): Natural and human causes and implications for water resources, ecosystems, economy, and society. *Water Resources Research*, *49*(2), 1040–1057. https://doi.org/10.1002/wrcr.20123

Wang, S., et al. (2015), Global-Scale Evaluation of Roughness Effects on C-Band AMSR-E Observations. *Remote Sensing, 7(5),* 5734–5757. https://doi.org/10.3390/rs70505734

Yang, K., Watanabe, T., Koike, T., Li, X., Fujii, H., Tamagawa, K., Ma, Y. & Ishikawa, H. (2007), Auto-calibration System Developed to Assimilate AMSR-E Data into a Land Surface Model for Estimating Soil Moisture and the Surface Energy Budget, *Journal of the Meteorological Society of Japan, 85A,* 229–242. https://doi.org/10.2151/jmsj.85A.229

Yang, K., Koike, T., Kaihotsu, I., & Qin, J. (2009). Validation of a Dual-Pass Microwave Land Data Assimilation System for Estimating Surface Soil Moisture in Semiarid Regions., *Journal of Hydrometeorology, 10(3)*, 780–793. https://doi.org/10.1175/2008JHM1065.1

Zhou, L., et al. (2014). Widespread decline of Congo rainforest greenness in the past decade. *Nature*, *509*(7498), 86–90. https://doi.org/10.1038/nature13265

Zhu, Z. et al. (2013), Global Data Sets of Vegetation Leaf Area Index (LAI)3g and Fraction of Photosynthetically Active Radiation (FPAR)3g Derived from Global Inventory Modeling and Mapping Studies (GIMMS) Normalized Difference Vegetation Index (NDVI3g) for the Period 1981 to 2011., *Remote Sensing, 5,* 927-948, https://doi.org/10.3390/rs5020927.

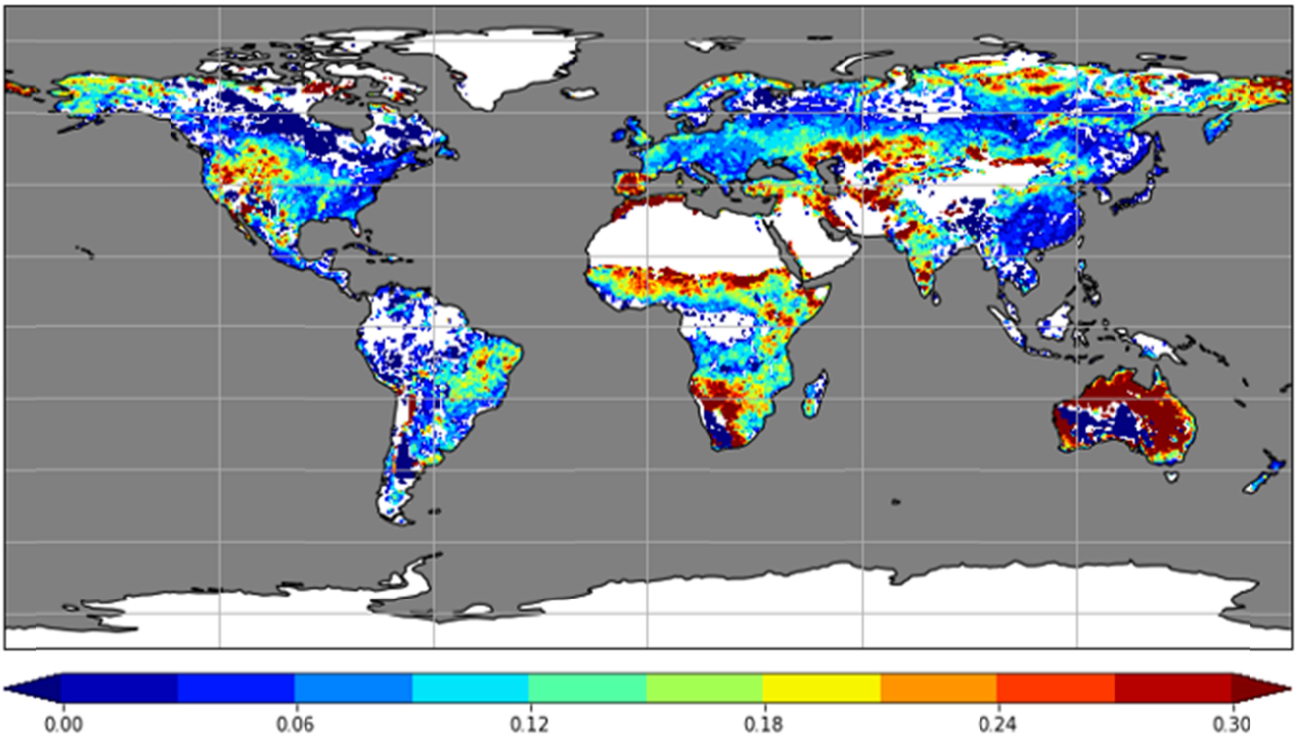

409

410 **Figure 1.** Climatologic b/y [-] (see section 3). Pixels which show a statistically significant slope between

411 microwave VOD and optical LAI (student's t-test, $p<0.05$) are depicted.

412

413

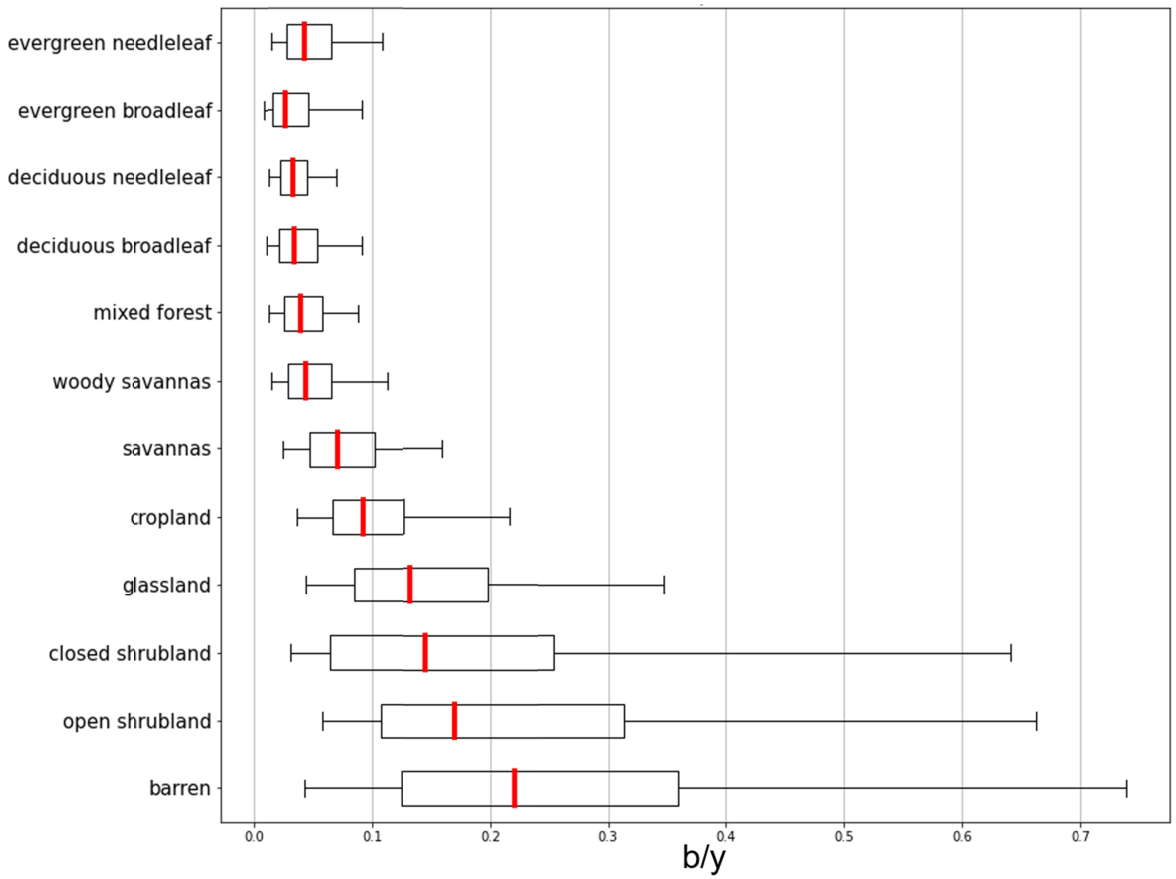

414

415 **Figure 2.** Boxplots of yearly b/y [-] (see section 3) stratified by land cover types. Pixels of water, wetland,

416 urban, mosaic, and ice are excluded.

417

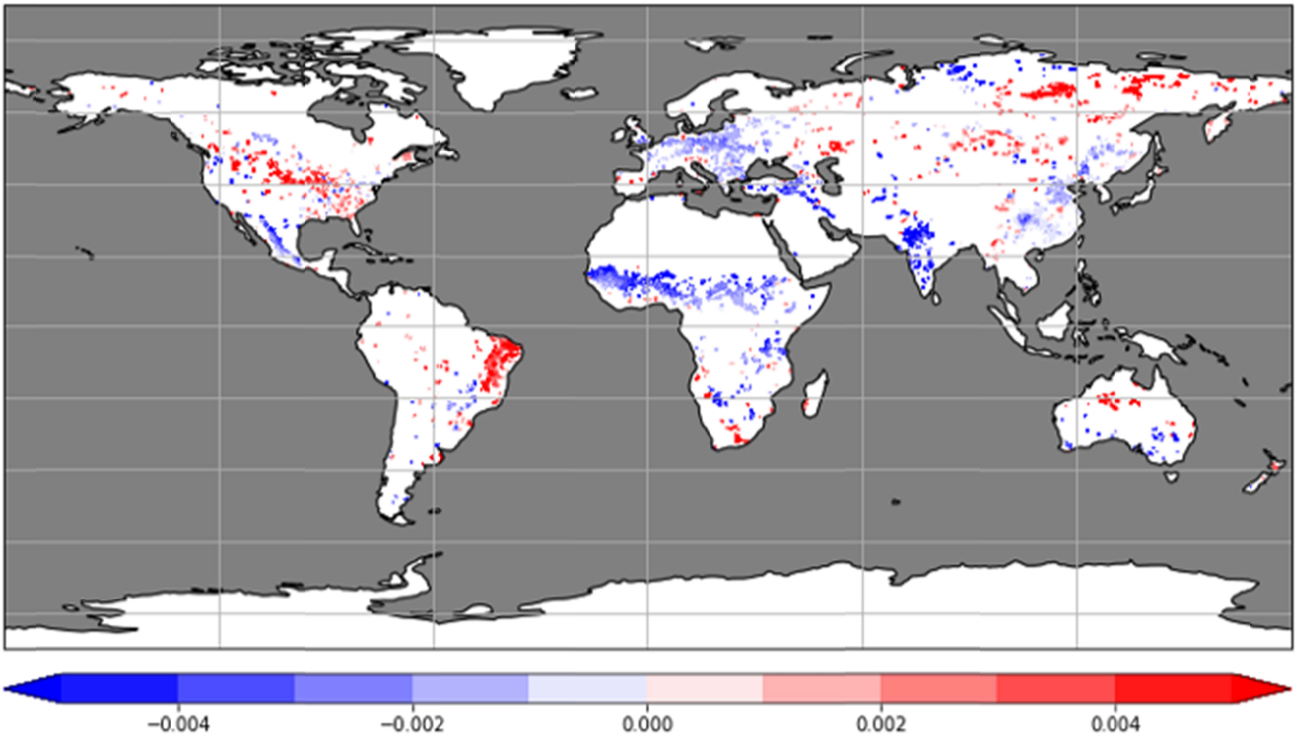

418

419 **Figure 3.** Linear trend of b/y [-] (see section 3) from 2003 to 2019. Pixels which show a statistically

420 significant trend (student's t-test, $p<0.05$) are depicted.